

AD-756 520

IMPATT DIODE AMPLIFIER

Charles Thomas Key

Naval Postgraduate School
Monterey, California

December 1972

DISTRIBUTED BY:

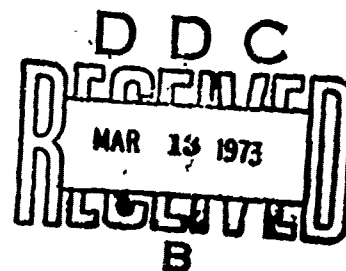
NTIS

National Technical Information Service
U. S. DEPARTMENT OF COMMERCE
5285 Port Royal Road, Springfield Va. 22151

AD 756520

NAVAL POSTGRADUATE SCHOOL

Monterey, California



THESIS

IMPATT DIODE AMPLIFIER

by

Charles Thomas Key

Thesis Advisor:

J. B. Knorr

December 1972

Approved for public release; distribution unlimited.

36

UNCLASSIFIED

Security Classification

DOCUMENT CONTROL DATA - R & D

(Security classification of title, body of abstract and indexing annotation must be entered when the overall report is classified)

1. ORIGINATING ACTIVITY (Corporate author) Naval Postgraduate School Monterey, California 93949		2a. REPORT SECURITY CLASSIFICATION Unclassified	
		2b. GROUP	
3. REPORT TITLE IMPATT DIODE AMPLIFIER			
4. DESCRIPTIVE NOTES (Type of report and, inclusive dates) Master's Thesis; December 1972			
5. AUTHOR(S) (First name, middle initial, last name) Charles T. Key; Lieutenant, United States Navy			
6. REPORT DATE December 1972		7a. TOTAL NO. OF PAGES 36	7b. NO. OF REFS 6
8a. CONTRACT OR GRANT NO.		8b. ORIGINATOR'S REPORT NUMBER(S)	
b. PROJECT NO.			
c.		9b. OTHER REPORT NO(S) (Any other numbers that may be assigned this report)	
d.			
10. DISTRIBUTION STATEMENT Approved for public release; distribution unlimited.			
11. SUPPLEMENTARY NOTES		12. SPONSORING MILITARY ACTIVITY Naval Postgraduate School Monterey, California 93940	
13. ABSTRACT A high performance IMPATT diode test circuit has been developed which is very effective in reducing spurious oscillations of the diode under test by controlling the impedance presented to the diode by the circuit. In this circuit, a 10 GHz silicon diode has been tested as an amplifier with power gains in excess of 20 db.			

DD FORM 1473 (PAGE 1)
1 NOV 66
S/N 0101-807-6811UNCLASSIFIED
Security Classification

A-81408

IMPATT Diode Amplifier

by

Charles Thomas Key
Lieutenant, United States Navy
B.S.E.E., University of Texas, 1965

Submitted in partial fulfillment of the
requirements for the degree of

MASTER OF SCIENCE IN ELECTRICAL ENGINEERING

from the
NAVAL POSTGRADUATE SCHOOL
December 1972

Author

Charles T. Key

Approved by:

Jeffrey B. Kuan

Thesis Advisor

Paul C. Cooper, acting
Chairman, Department of Electrical Engineering

Milton H. Danner
Academic Dean

ABSTRACT

A high performance IMPATT diode test circuit has been developed which is very effective in reducing spurious oscillations of the diode under test by controlling the impedance presented to the diode by the circuit. In this circuit, a 10 GHz silicon diode has been tested as an amplifier with power gains in excess of 20 db.

TABLE OF CONTENTS

I.	INTRODUCTION -----	6
II.	CIRCUIT DESIGN -----	7
	A. DIODE MOUNT -----	7
	B. TRANSFORMER -----	8
	C. BIAS-T -----	10
III.	PRESENTATION OF DATA -----	16
IV.	CONCLUSION -----	25
	APPENDIX A: ASSEMBLY OF IMPATT AMPLIFIER -----	27
	COMPUTER PROGRAM -----	30
	BIBLIOGRAPHY -----	33
	INITIAL DISTRIBUTION LIST -----	34
	FORM DD 1473 -----	35

LIST OF FIGURES

Figure

1.	Three-section Chebyshev Transformer -----	8
2.	Circuit Dimensions for Microstrip Bias-T -----	11
3.	Microstrip Bias T Power Transmission Properties into 50 Ω Load -----	12
4.	Square of Reflection Coefficient for Microstrip Bias T vs. Frequency -----	13
5.	Disassembled IMPATT Diode Amplifier -----	14
6.	Microstrip 'Bias-T' Connected to Diode Amplifier with APC-7 Connector -----	15
7.	Block Diagram of Reflection Amplifier Swept Measurement Circuit -----	16
8.	Frequency Response of Amplifier for $P_{IN} = -20$ dbm -----	17
9.	Frequency Response of Amplifier for $P_{IN} = -15$ dbm -----	18
10.	Frequency Response of Amplifier for $P_{IN} = -10$ dbm -----	18
11.	Frequency Response of Amplifier for $P_{IN} = -5$ dbm -----	19
12.	Frequency Response of Amplifier for $P_{IN} = 0$ dbm -----	19
13.	Block Diagram of Reflection Amplifier CW Power Measurement Circuit -----	20
14.	P_{OUT} vs. P_{IN} for the Amplifier at Different Bias Currents (Diode #2) -----	21
15.	f_o vs. P_{IN} Corresponding to Figure 14 (Diode #2) -----	22
16.	P_{OUT} vs. P_{IN} for the Amplifier at Different Bias Currents (Diode #3) -----	22

17. f_o vs. P_{IN} Corresponding to Figure 16
(Diode #3) ----- 23
18. Diode Negative Resistance, R_D , Plotted as a
Function of the Diode RF Current Amplitude,
 I_D ----- 24

I. INTRODUCTION

The amplification of microwave power by the use of IMPATT diodes is presently stimulating increased interest of design engineers at all levels. IMPATT diodes are now commercially available and are being used in a variety of applications. The much improved manufacturing processes of these microwave devices in recent years has led to their increased reliability, efficiency, and noise suppression while cost has continually declined. With the rapid changes being made in the state-of-the-art of these microwave devices, high performance circuitry is required for use within a laboratory environment for purposes of testing the performance and checking the specifications of the many IMPATT diodes now offered commercially by many different vendors.

This paper describes the design and development of such circuitry along with the experimental procedures and measurement techniques involved in the testing of several Hewlett Packard type 5082-0432, 10 GHz, IMPATT diodes as amplifiers. The power gain, bandwidth, and frequency sensitivity of this type diode is presented in the form of curves to acquaint the reader with the principles of IMPATT diode amplification.

II. CIRCUIT DESIGN

A. DIODE MOUNT

An IMPATT diode can function as an amplifier if the load resistance presented to it is larger in magnitude than the diode's negative resistance. Where many diodes of different types are to be analyzed, the collet-clamp-sleeve design of Appendix A is especially suitable for end-mounting diodes in coaxial circuits and provides a convenient mount for a laboratory test fixture, where quick interchangeability of diodes and transformers is desirable. The diode holder assembly consists of four parts: A "collet" for gripping the heat sink end of the diode, a "sleeve" into which the diode collet is inserted, a "knurled nut" which pulls the collet tightly into the sleeve, and a "clamp." The clamp is screwed into the cavity body, and is tightened after the sleeve containing diode and collet has been inserted and held with moderate pressure against the coaxial transformer. This arrangement allows easy interchangeability of diodes and transformers and ensures a low electrical and thermal resistance contact between diode and cavity. Version "G" of the collet was used in this particular application. Figure 5 is a picture of the disassembled diode mount.

B. TRANSFORMER

The transformer reduces the $50\ \Omega$ line impedance to the value of load resistance (R_L) required for optimum power output of the IMPATT diode, usually in the vicinity of $2\ \Omega$. The transformer is a very critical part of the circuit design. The type of transformer used is a Chebyshev, quarter-wave, three-section design; this provides the optimum diode impedance over a wider frequency range than a transformer of maximally flat design and with the aid of the computer program on page 30 is no more difficult to design or build. The exact equations governing the design of the transformer are contained in Ref. 1. A description of what the computer program does can be explained with the aid of Fig. 1.

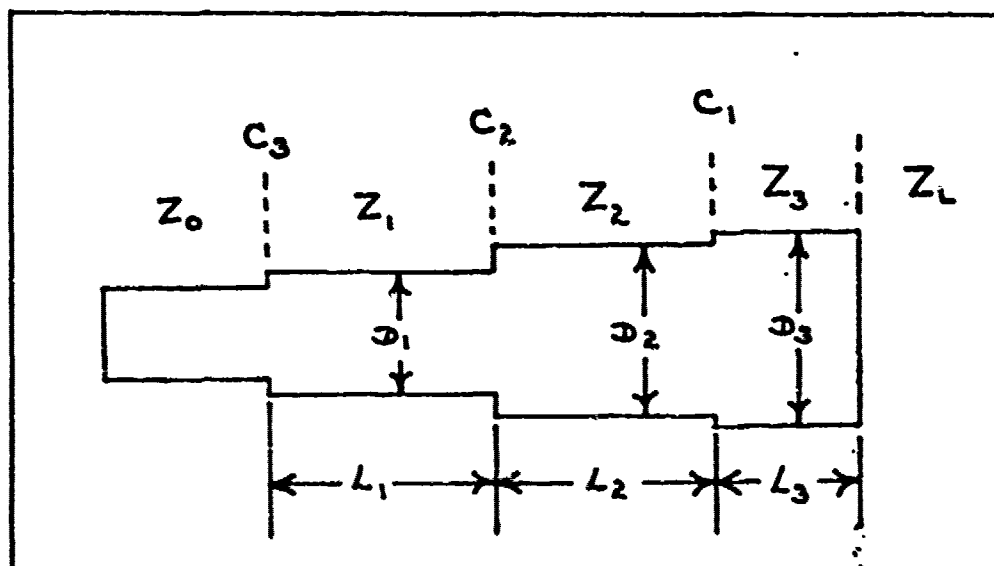


Figure 1. Three-section Chebyshev Transformer.

Given values for the line impedance (Z_0), a desired value of diode load impedance (Z_L), a center frequency, a desired bandwidth, and the relative dielectric constant of the material which surrounds the larger end of the transformer (Rexolite is recommended), the computer output will yield the appropriate diameters and lengths of the transformer sections.

In addition, the computer output will yield the necessary numerical ratios that are needed to determine the length corrections to the transformer sections which are necessitated by the capacitance associated with the discontinuity caused by each transformer step as described in Ref. 2. The values of these discontinuity step capacitances can be readily obtained from a graph in Ref. 2.

For optimum computer transformer design, these step capacitances must then be fed into the computer with a supplementary deck of cards. The final computer output then yields the diameters of the transformer sections along with the sections' lengths corrected for the discontinuity step capacitances. At high frequencies there can be as much as 5% length correction necessary to each transformer section.

Other computer outputs include the center frequency, transformer bandwidth, maximum reflection coefficient, line impedance, diode load impedance, quarter-wave length in free space, and quarter-wave length in the specified dielectric material.

The transformer which was used to analyze the HP 5082-0432 diode has the following design criteria:

$$Z_o = 50.0 \Omega$$

$$Z_L = 1.1 \Omega$$

$$f_o = 10.2 \text{ GHz}$$

$$\text{Bandwidth} = 1.2 \text{ GHz}$$

$$\text{Maximum reflection coefficient} = 0.0463$$

$$D_1 = 0.1665 \text{ in.}$$

$$D_2 = 0.2436 \text{ in.}$$

$$D_3 = 0.2626 \text{ in.}$$

$$L_1 = 0.2816 \text{ in.}$$

$$L_2 = 0.2785 \text{ in.}$$

$$L_3 = 0.1806 \text{ in.}$$

C. BIAS T

A Bias T is required for operation of the amplifier cavity. The diode requires a DC bias current, typically 30 mA for the HP 5082-0432 diode. It is necessary to block the DC bias current from the rest of the circuitry. This has been accomplished using a microstrip interdigital DC blocking capacitor circuit derived from design criteria presented in Ref. 3. The microstrip circuit is shown in Fig. 2.

The circuit was designed for a center frequency of 9.8 GHz and was constructed on 0.030 inch copper substrate with a ratio of free space wavelength to microstrip wavelength equal to 1.44. The two "fingers" in Fig. 2

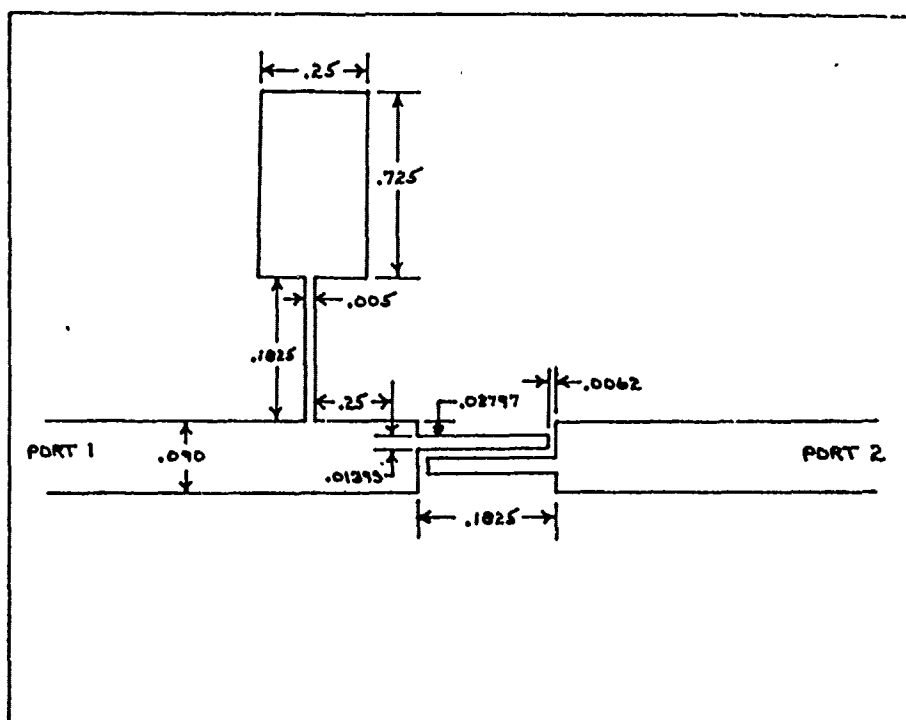


Figure 2. Circuit Dimensions for Microstrip Bias T.

represent the DC blocking capacitor and have a coupling length equal to a quarter-wavelength in microstrip.

The DC bias current is applied to the diode through a very high rf impedance (quarter-wavelength long, very narrow piece of copper) terminated in a low rf impedance (wide piece of copper). This arrangement serves as a very effective "bucket choke" to rf energy passing from PORT 1 to PORT 2 or vice-versa.

The transmission properties of the microstrip Bias T are shown in Figs. 3 and 4. Figure 3 indicates the amount of relative power that is reflected from PORT 1 or PORT 2 when the indicated incident power is applied to the same port and the other port is terminated in a 50Ω load.

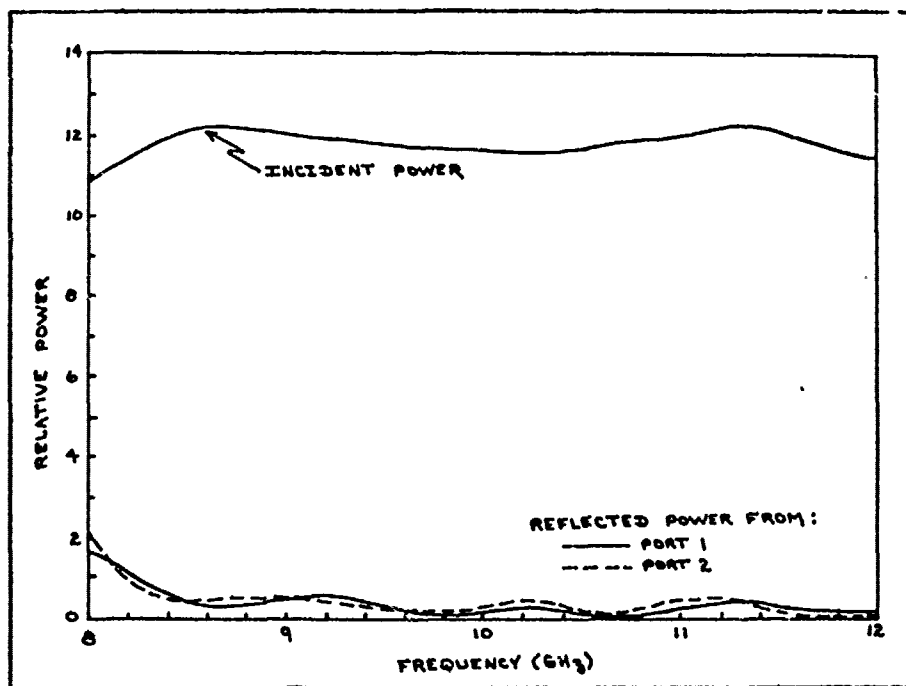


Figure 3. Microstrip Bias T Power Transmission Properties into 50 Ω Load.

Figure 4 was readily obtained from the curves of Fig. 3 and indicates the square of the reflection coefficient for the microstrip Bias T at each port. It is seen that in the frequency range from 9.6 to 11.0 GHz that less than 2% of the incident power is reflected from PORT 1 and less than 4% of the incident power is reflected from PORT 2. The VSWR over the frequency range of 8.5 to 12.0 GHz has a maximum of 1.54 at a frequency of 9.2 GHz looking into PORT 1 and is considerably less at both ports over most of that frequency range. The transmission properties at frequencies higher than 12 GHz were not determined as measurement equipment above 12 GHz was not available, but extrapolation

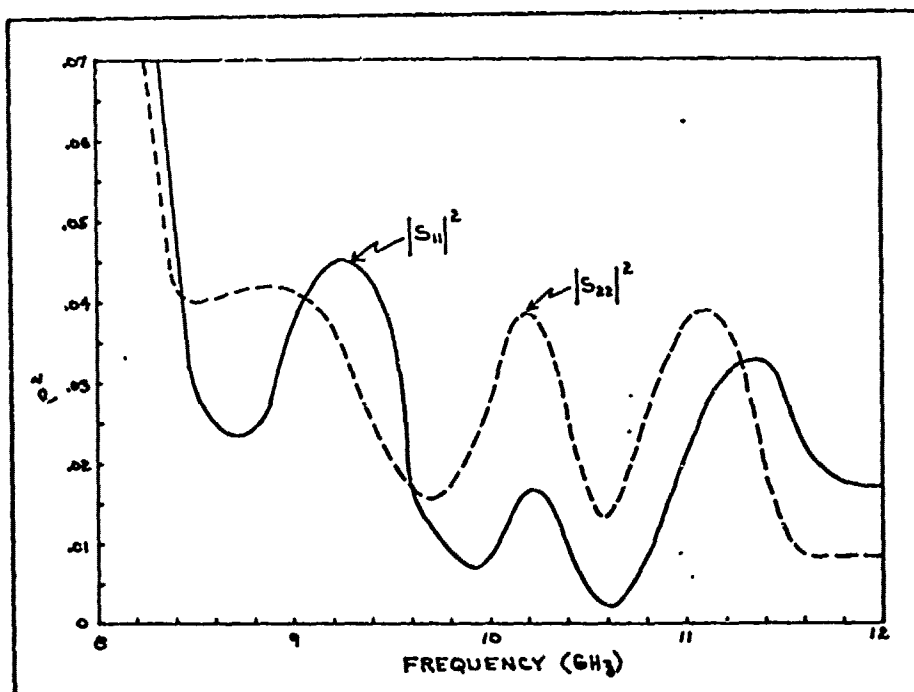


Figure 4. Square of Reflection Coefficient for Microstrip Bias T vs. Frequency.

of the curves to higher frequencies seems very encouraging toward low VSWR, very broadband Bias T's of this design.

Figure 6 is a picture of the microstrip Bias T connected to the diode amplifier by an Amphenol APC-7 connector.

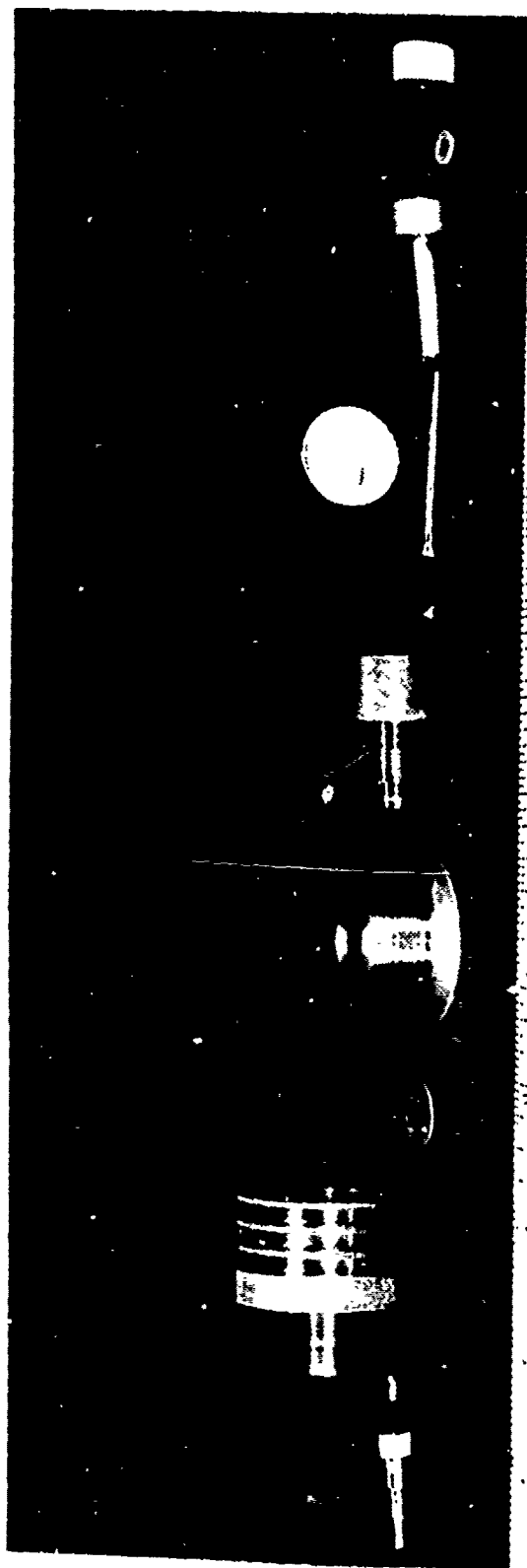


Figure 5. Disassembled IMPATT Diode Amplifier.

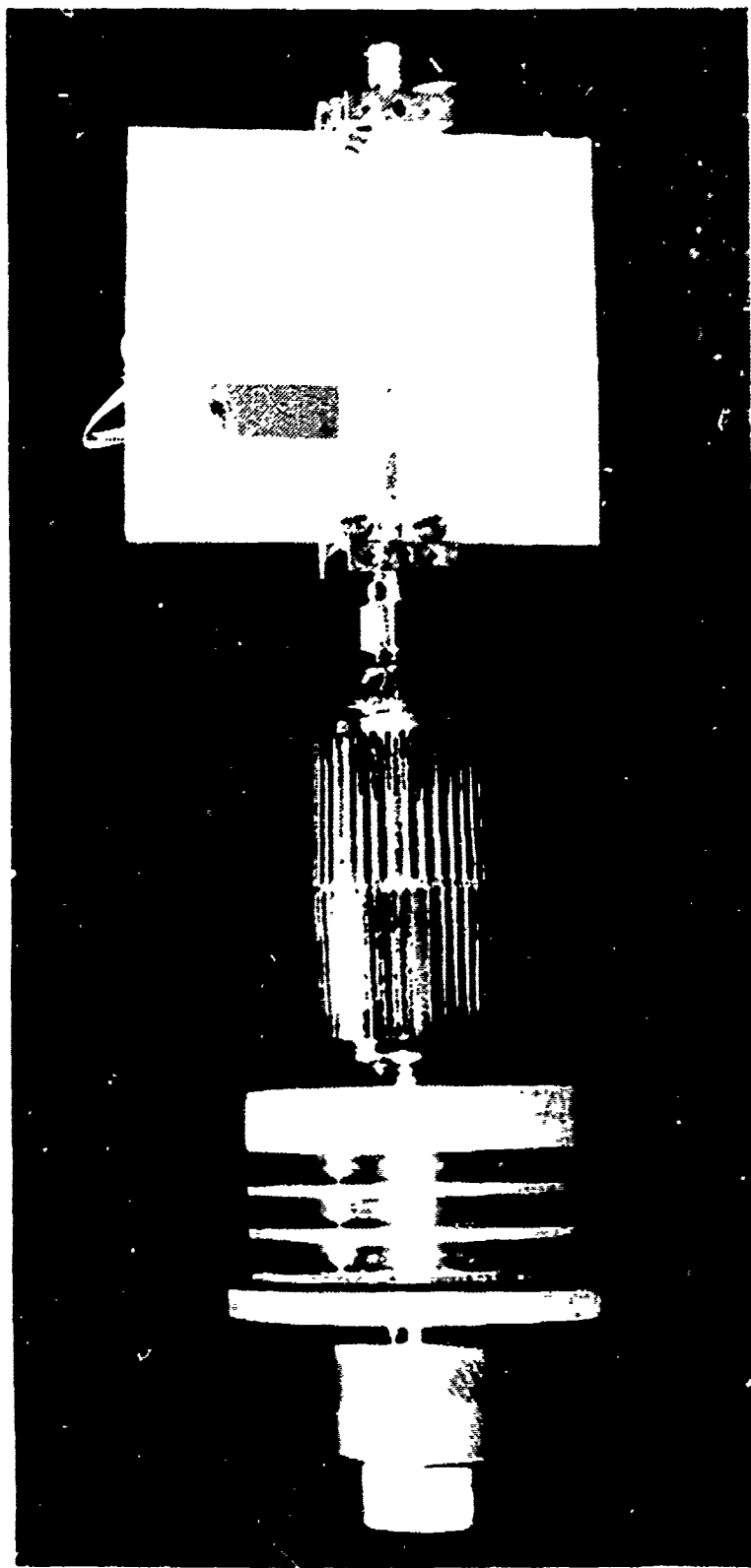


Figure 6. Microstrip 'Bias-T' Connected to Diode Amplifier with APC-7 Connector.

III. PRESENTATION OF DATA

Figure 7 shows the block diagram of the IMPATT reflection amplifier swept measurement circuit. A circulator is used to separate input and output signals. The HP Model 8472A crystal detector operates within square law up to 100 mW of input power to the detector. When connected to an oscilloscope, the diode's frequency response can be quickly ascertained. The maximum possible dc bias current above which the diode breaks into oscillations can be readily observed also.

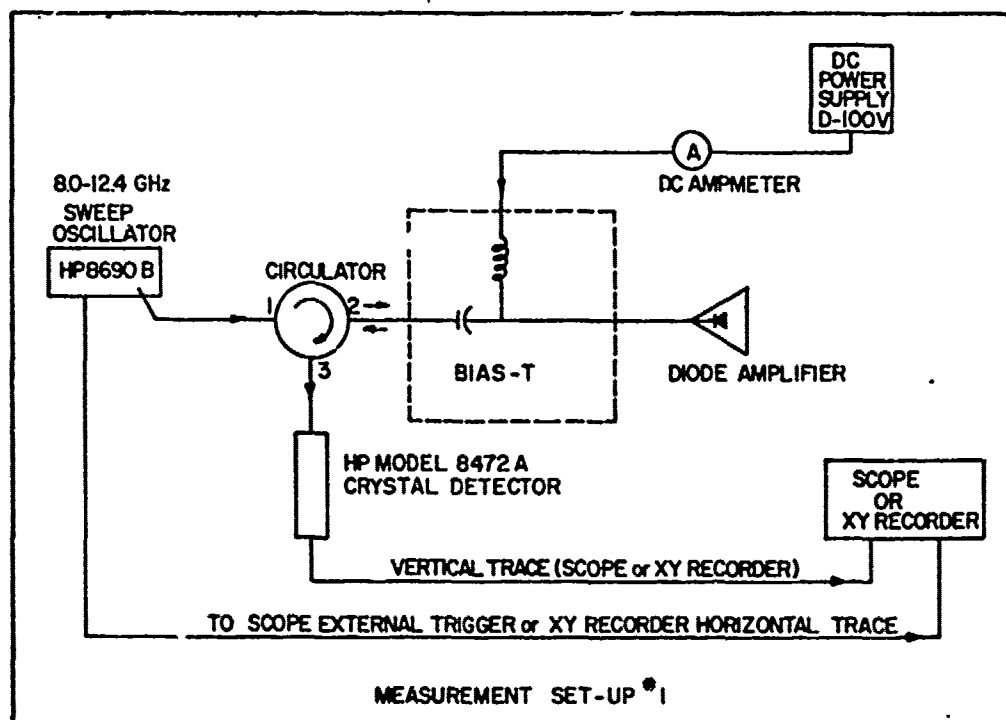


Figure 7. Block Diagram of Reflection Amplifier Swept Measurement Circuit.

Figures 8-12 were obtained on an X-Y recorder and represent one particular diode's swept frequency response for different input power levels and dc bias currents. All of the diodes tested had slightly different frequency responses and maximum dc bias currents, but in general they all exhibited the same characteristics of tending toward saturation with increasing input power levels and a corresponding increase in bandwidth. There is also a frequency shift of the center frequency toward lower frequencies with increasing input power levels or decreasing dc bias currents.

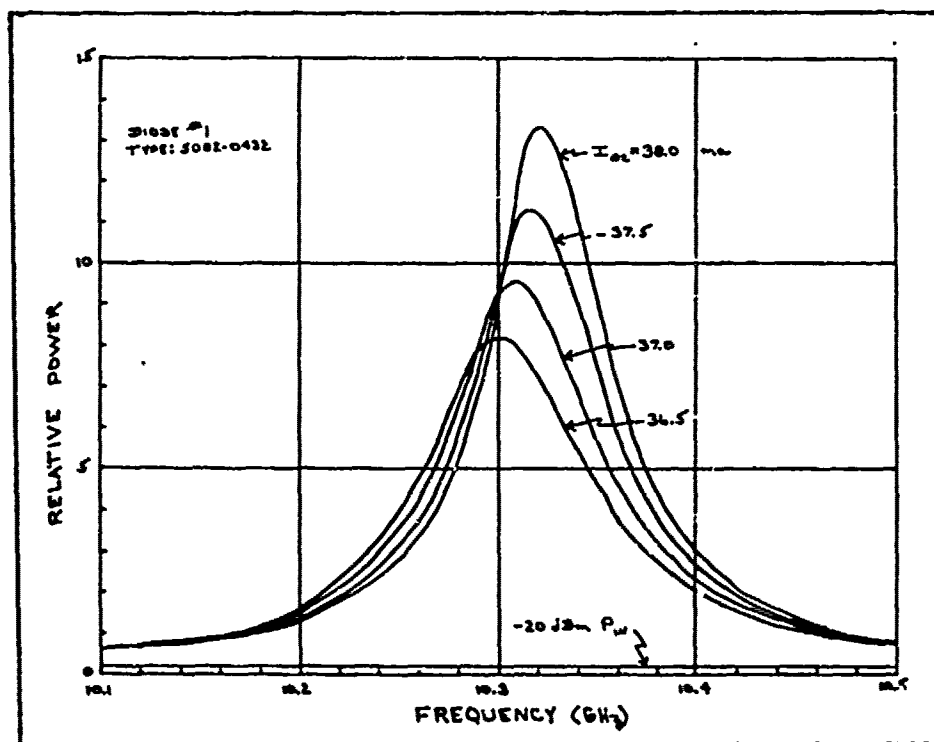


Figure 8. Frequency Response of Amplifier for $P_{IN} = -20$ dbm.

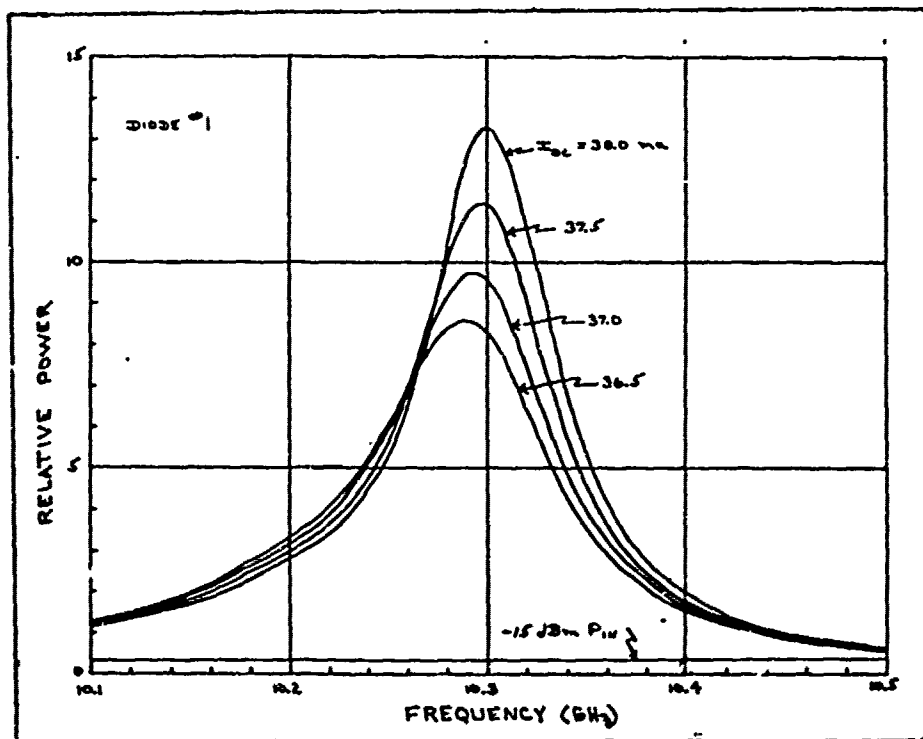


Figure 9. Frequency Response of Amplifier
for $P_{IN} = -15$ dbm.

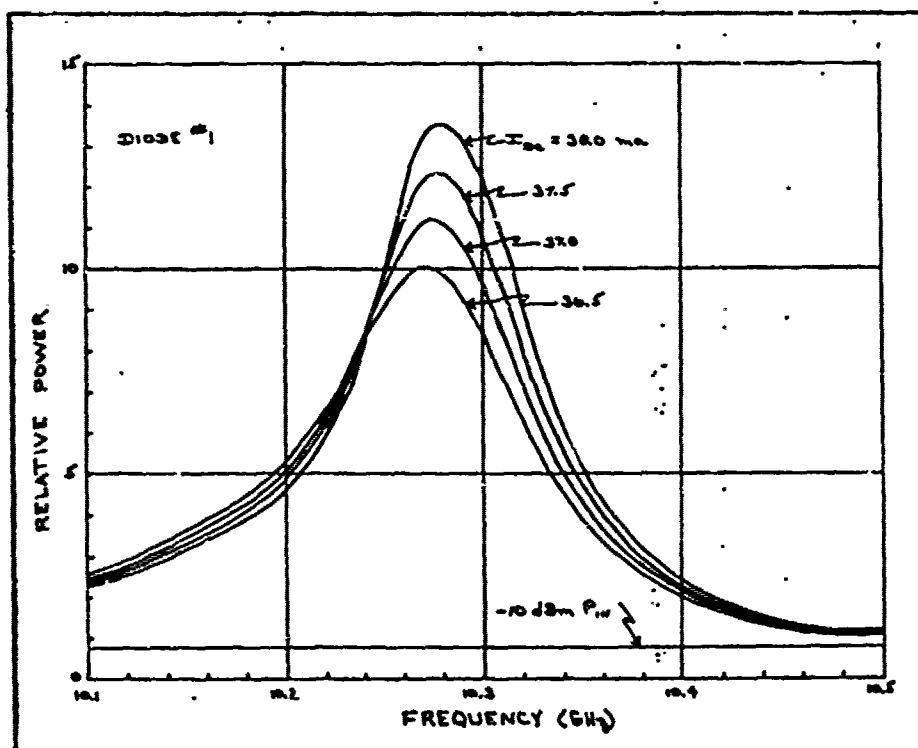


Figure 10. Frequency Response of Amplifier
for $P_{IN} = -10$ dbm.

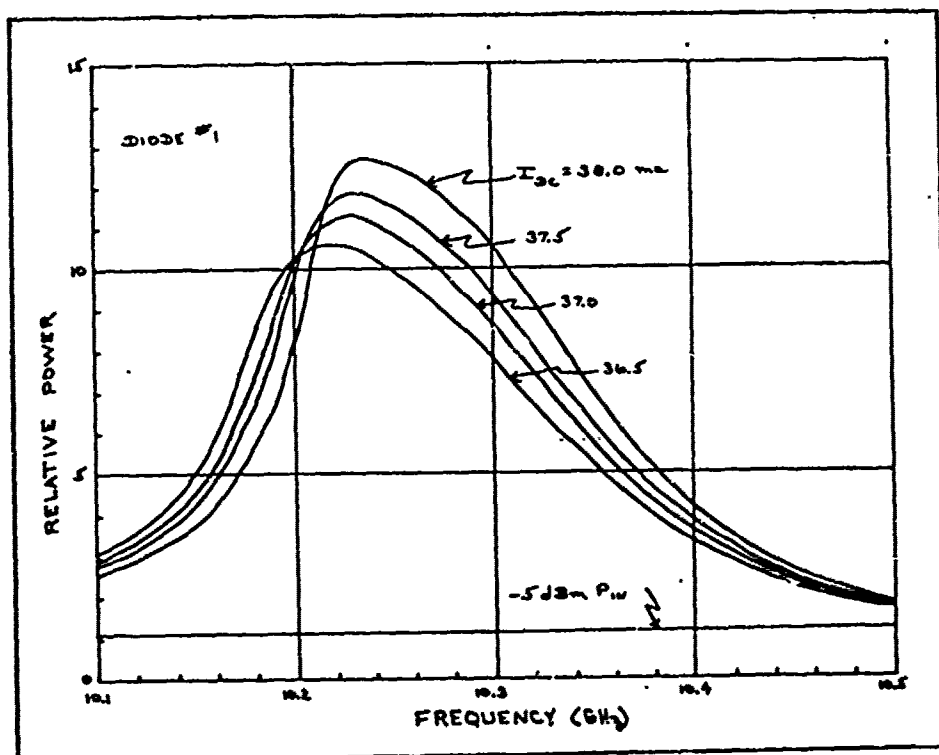


Figure 11. Frequency Response of Amplifier for $P_{IN} = -5$ dbm.

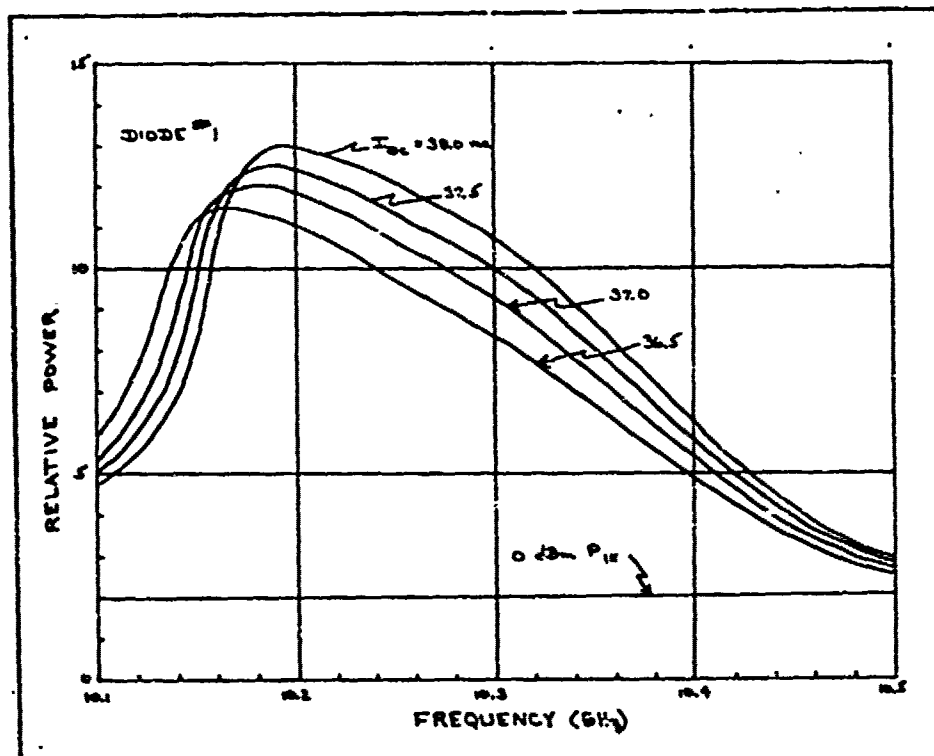


Figure 12. Frequency Response of Amplifier for $P_{IN} = 0$ dbm.

Figure 13 shows the block diagram of the IMPATT reflection CW power measurement circuit that was used. The location of two HP 432A power meters, as shown, enables the simultaneous measurement of input and output power for the diode under test. The 10 db directional coupler was calibrated for accuracy in measuring the input power. The CW frequency of the HP 8690B was adjusted to coincide with the center operating frequency, as determined from the peak of the frequency response curves of the diode under test, for each different value of bias current and input power level. Output power vs. input power data and the

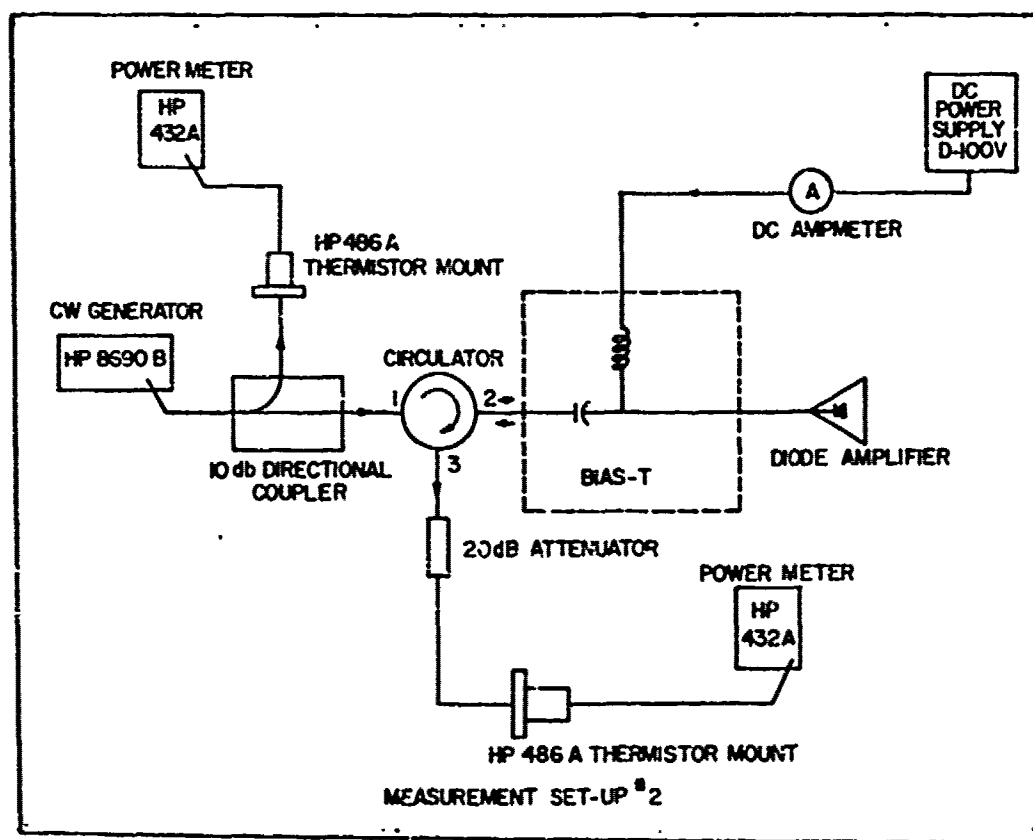


Figure 13. Block Diagram of Reflection Amplifier CW Power Measurement Circuit.

corresponding center frequencies where the measurements were made are shown for two different diodes and various values of bias current in Figures 14-17.

At the center frequency, the power gain of the amplifier is given by

$$G_o = \left[\frac{R_D - R_L}{R_D + R_L} \right]^2 \quad (1)$$

where R_D is the terminal (negative) resistance of the packaged diode and R_L is the diode's load resistance. An estimate for the power added by the amplifier is given by

$$P_A \approx \frac{1}{2} I_D^2 |R_D| \quad (2)$$

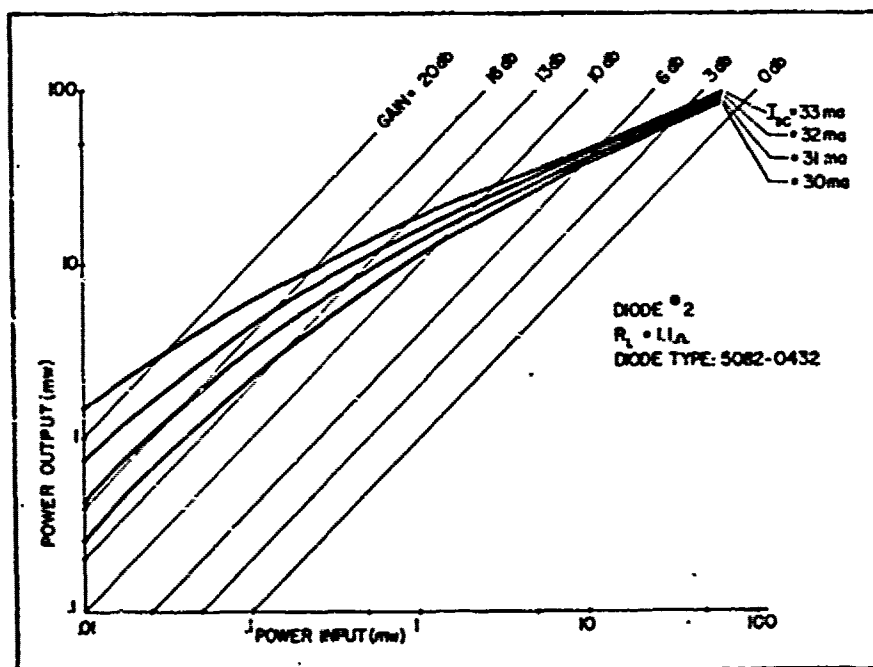


Figure 14. P_{OUT} vs. P_{IN} for the Amplifier at Different Bias Currents (Diode #2).

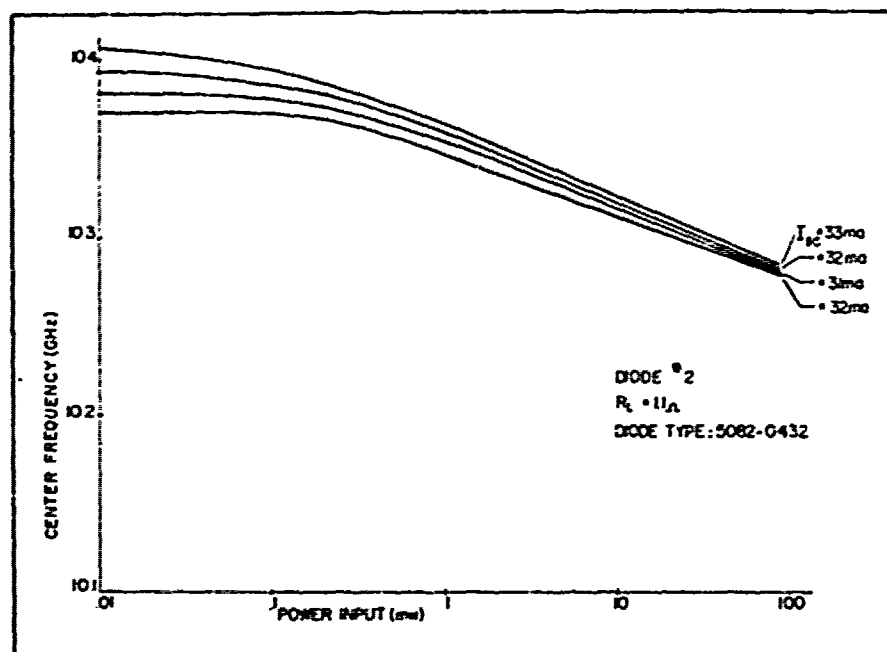


Figure 15. f_0 vs. P_{IN} Corresponding to Figure 14 (Diode #2).

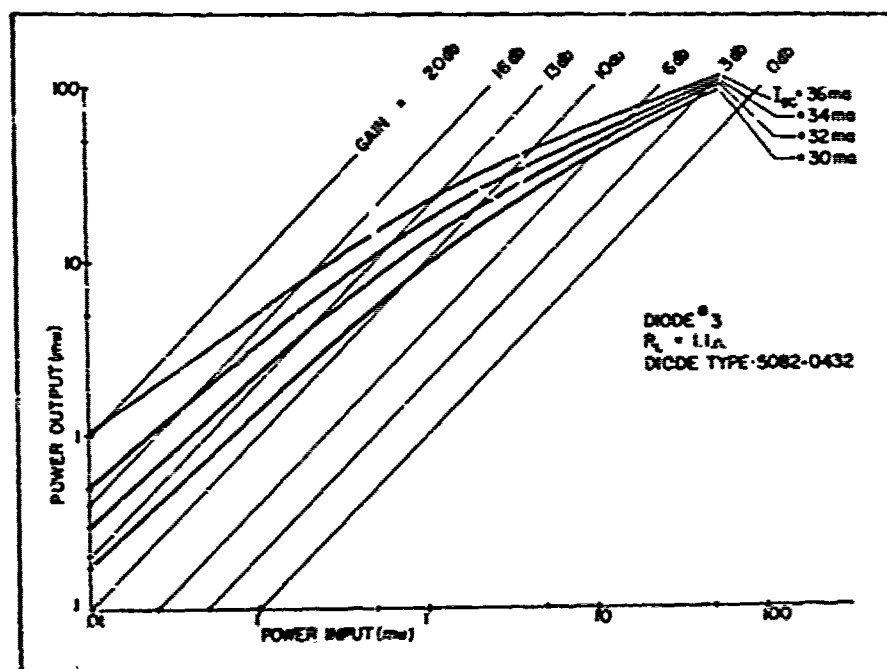


Figure 16. P_{OUT} vs. P_{IN} for the Amplifier at Different Bias Currents (Diode #3).

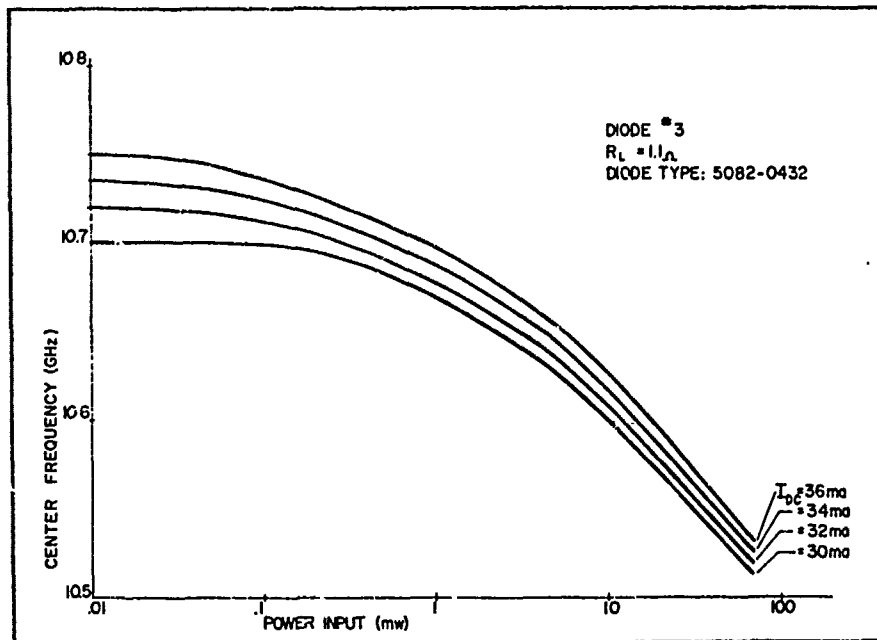


Figure 17. f_o vs. P_{IN} Corresponding to Figure 16 (Diode #3).

where I_D is the diode's RF current amplitude. R_D may be determined from equation (1) with the use of the power gain curves shown in Figs. 14 and 16. I_D may be estimated from equation (2) by using the same power gain curves. Figure 18 shows how the diode negative resistance typically varies as a function of the diode RF current amplitude.

It is seen that $|R_D|$ decreases with signal level. R_D also varies with dc bias current and thus the upper limit of bias current is established at the value that causes $|R_D|$ to equal R_L . Exceeding this maximum value of bias current will cause the diode to act as an oscillator instead of an amplifier because the diodes load resistance, R_L , is no longer greater than the magnitude of the diode's negative resistance, $|R_D|$.

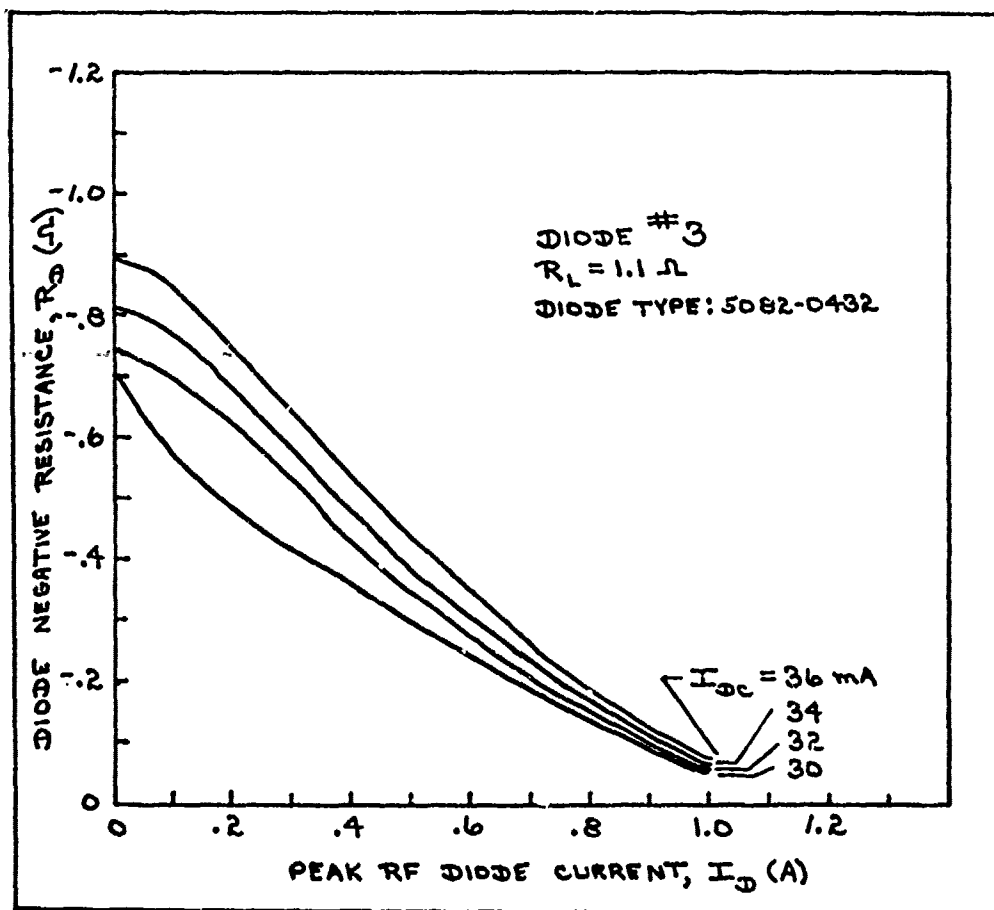


Figure 18. Diode Negative Resistance, R_D , Plotted as a Function of the Diode RF Current Amplitude, I_D .

IV. CONCLUSION

An IMPATT amplifier requires that R_L be larger than $|R_D|$ for all values of the RF current through the diode. Since R_D varies not only with different types of diodes, but also with dc bias current and signal level, the selection of R_L for optimum power gain is of prime importance in the design of the amplifier. Measurements of reflection amplifier characteristics allow the determination of the R_D vs. I_D curve for a diode which enhances the selection of the optimum R_L . A three-step Chebyshev transformer which is designed with consideration of the coaxial line-step fringing capacities provides the optimum R_L over a wider frequency range than a transformer of any other design.

Depending upon the exact circumstances, final adjustment of the circuit inductance to achieve the desired center frequency, is usually a cut-and-try process. One technique is to recess the diode deeper into the "collet" as shown by the different versions of collet design in Appendix A. Recessing the diode deeper into the collet has the effect of lowering the circuit inductance and raising the frequency.

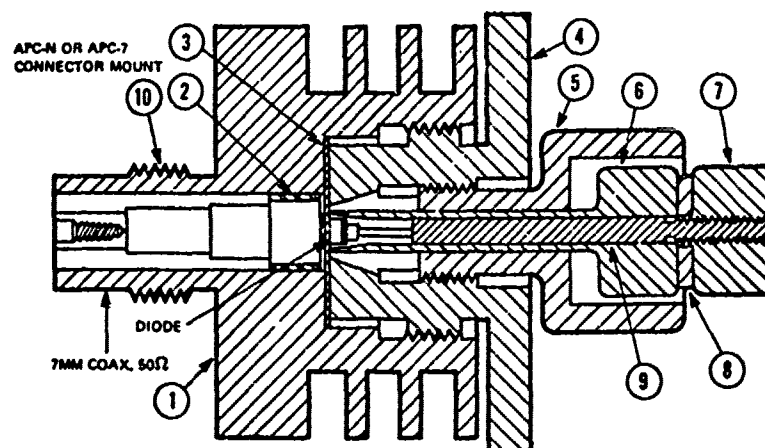
The low power Hewlett Packard type 5082-0432 IMPATT diodes that were tested as amplifiers exhibited power gains in excess of 20 db with bandwidths on the order of 30 MHz at input power levels of about 0.01 mW. At input power levels of 100 mW, they approach saturation, but their bandwidths

tend toward infinity. The maximum power added by the diode occurs somewhere between these two extremes and is on the order of 50 mW.

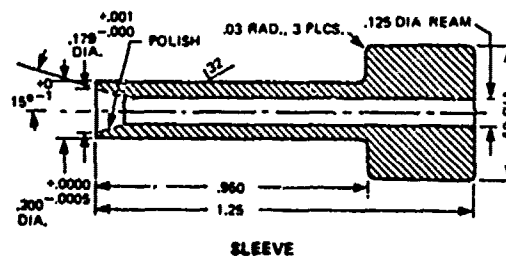
The gain-bandwidth-power added requirements of an amplifier are therefore important design specifications. The selection of the type of diode to be used and its biasing conditions will be of interest to design engineers depending on what purpose the amplifier is to be used. Because of their small size, weight, low heat output, high gain, and wide bandwidth characteristics, IMPATT diode amplifiers are accordingly very attractive for many applications, including those which are price-sensitive.

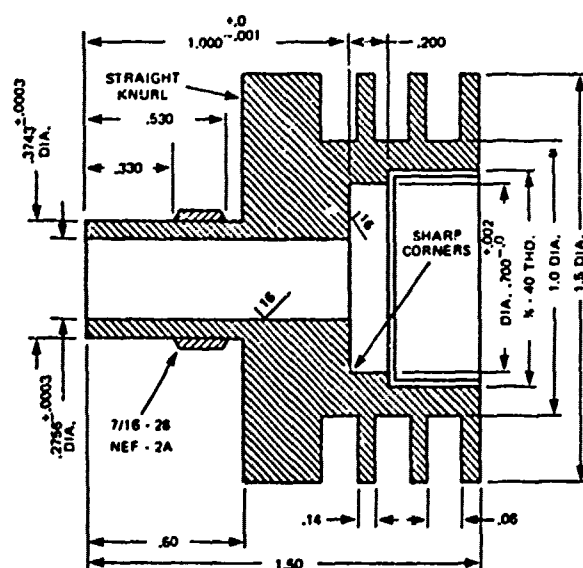
APPENDIX A

ASSEMBLY OF IMPATT AMPLIFIER

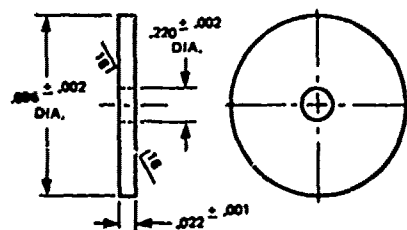


ITEM	DESCRIPTION	MFG. PART NO.
10	CONNECTOR ASS'Y	AMPHENOL ≈ 131-1050 (APC-7) ≈ 131-10004 (APC-N)
9	COLLET, VERSION G	
8	WASHER ≈ 4	
7	NUT	
6	SLEEVE	
5	CLAMP	
4	NUT	
3	SPACER	
2A	BEAD (TRANSFORMER)	
2	TRANSFORMER	
1	CAVITY BODY	

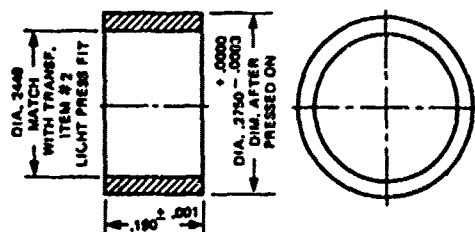




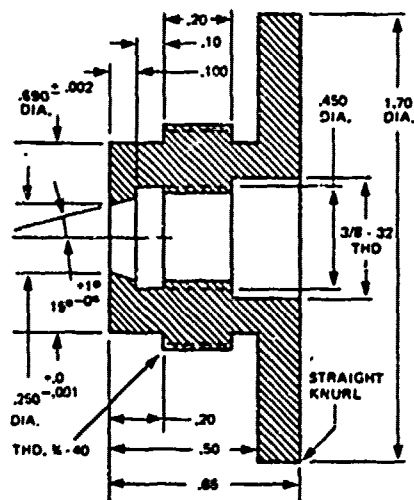
CAVITY BODY



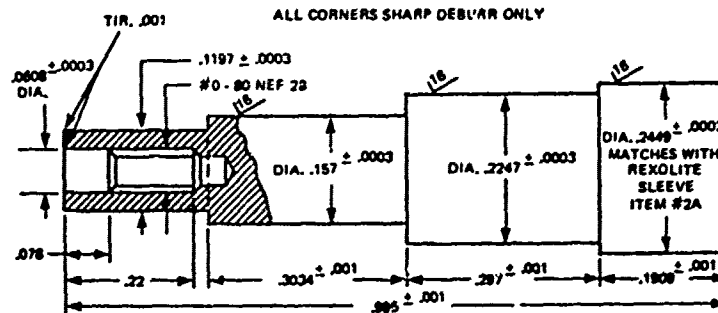
SPACER



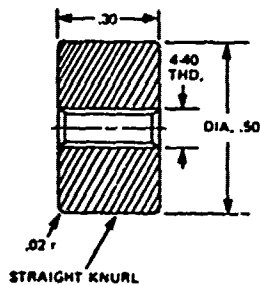
BEAD (TRANSFORMER)



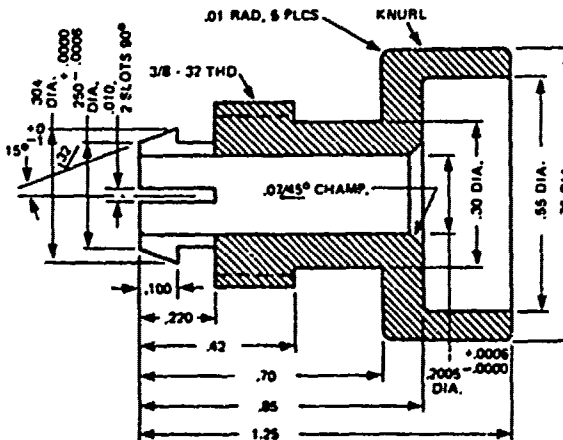
NUT



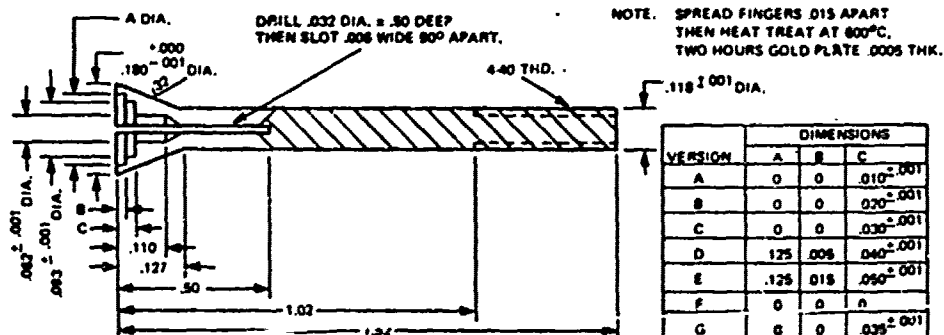
TRANSFORMER



NUT



CLAMP



COLLET

COMPUTER PROGRAM

OPTIMUM CHEBYSHEV THREE SECTION STEPPED TRANSFORMER

NOTE: 5 DATA CARDS REQUIRED IN MAIN DECK ARE AS FOLLOWS:

- (1) FREQ = FREQUENCY IN GIGAHERTZ
- (2) BW = BANDWIDTH IN GIGAHERTZ
- (3) ZL = LOAD IMPEDANCE IN OHMS
- (4) ZO = CHARACTERISTIC IMPEDANCE IN OHMS
- (5) ER = RELATIVE DIELECTRIC CONSTANT OF REXOLITE

NOTE: ZO MUST BE GREATER THAN ZL

```

FREQ = 10.2
BW = 1.2
ZL = 1.1
ZO = 50.0
ER = 2.54
RAD1 = 0.1378
PI = 3.14159
HALFPI = PI/2.0
THOPI = 2.0 * PI
AM = HALFPI - (PI * BW)/(4.0 * FREQ)
AZ = ARCOS((SQRT(3.0)/2.0) * COS(AM))
X = ((ZO - ZL) ** 2.0) * 2.0 * COS(AZ)
Y = 4.0 * ZL * ZO * 3.0 * SQRT(3.0) * (TAN(AZ) ** 2.0)
S = X/Y
PM = SQRT(S/(S + 1.0))
F1 = (AM/HALFPI) * FREQ
F2 = (2.0 - AM/HALFPI) * FREQ
RHO1 = (AZ/HALFPI) * FREQ
RHO2 = (2.0 - AZ/HALFPI) * FREQ
ANS = (ZL - ZO)/(TAN(AZ) ** 2.0)
ALFA = 0.124
A = 2.0 * SQRT(ZL/ZO)
B = ZL * (ZO ** 2.0)
C = A * (ZO ** 2.0)
10 ALFA = ALFA + 0.001
30 BETA = 1.0 - ALFA
Z1 = (ZL ** ALFA) * (ZO ** BETA)
CHECK = ((Z1 ** 2.0)/ZO) + (A * Z1) - (B/(Z1 ** 2.0)) - (C/Z1)
TOL = ABS(CHECK)
IF (TOL.LE.0.0002) GO TO 10
IF (TOL.GT.0.0001) GO TO 50
GO TO 75
50 ALFA = ALFA - 0.00005
GO TO 30
75 Z2 = SQRT(ZL * ZO)
Z3 = (ZL * ZO)/Z1
WAVE1 = 30.0/(4.0 * FREQ * 2.54)
WAVE2 = WAVE1/SQRT(ER)
T = THOPI/377.0
D1 = 2.0 * (RAD1/EXP(T * Z1))
D2 = 2.0 * (RAD1/EXP(T * Z2))
D3 = 2.0 * (RAD1/EXP(T * Z3 * SQRT(ER)))
D0 = 0.1197
T1 = (RAD1 - D3/2.0)/(RAD1 - D2/2.0)
T2 = (RAD1 - D2/2.0)/(RAD1 - D1/2.0)
T3 = (RAD1 - D1/2.0)/(RAD1 - D0/2.0)
T11 = RAD1/(D2/2.0)
T22 = RAD1/(D1/2.0)
T33 = RAD1/(D3/2.0)
WRITE (6,100) FREQ
WRITE (6,200) BW
WRITE (6,300) PM
WRITE (6,400) F1,RHO1,FREQ,RHO2,F2
WRITE (6,500) WAVE1,WAVE2
WRITE (6,600) Z1,Z2,Z3,ZL
WRITE (6,700) D1,D2,D3
    
```

```

WRITE (6,800) TOL
WRITE (6,900) ALFA
WRITE (6,905) T11,T22,T33,T1,T2,T3
100 FORMAT (1H1,10X,'THE CENTER FREQUENCY IN GIGAHERTZ IS',
      8X,F7.4//)
200 FORMAT (11X,'THE BANDWIDTH IN GIGAHERTZ IS',14X,F8.4//
      /)
300 FORMAT (11X,'THE MAXIMUM REFLECTION COEFFICIENT IS',6X
      F8.4//)
400 FORMAT (11X,'CRITICAL FREQUENCIES ARE'//18X,'F(LOW)',1
      0X,'RHO1',11
      *X,'F(CENTER)',9X,'RHO2',10X,'F(UP)'//7X,5F16.3//)
500 FORMAT(11X,'QUARTER-WAVE LENGTH (INCHES) IN FREE SPACE
      IS',5X,F10.
      *8//11X,'QUARTER-WAVE LENGTH (INCHES) IN REXOLITE IS',
      7X,F10.8//)
600 FORMAT (11X,'THE IMPEDANCE OF THE TRANSFORMER SECTIONS
      IN OHMS ARE
      *//20X,'Z0',12X,'Z1',12X,'Z2',12X,'Z3',12X,'ZL'//11X,5
      =14.5//)
700 FORMAT (11X,'THE DIAMETERS OF THE TRANSFORMER SECTIONS
      ARE'//20X,'
      *D1',12X,'D2',12X,'D3'//10X,3F14.5//)
800 FORMAT (11X,'THE TOLERANCE OF THIS CALCULATION IS',F14
      .8//)
900 FORMAT (11X,'ALFA IS EQUAL TO',F10.5//)
905 FORMAT (11X,'THE RATIOS NECESSARY TO FIND DISCONTINUITY
      CAPACITANCES FROM GRAPHS BY J. WHINNERY'//20X,'R11',12X,'R22',12
      X,'R33'//11X
      *,3F14.3//20X,'R1',13X,'R2',13X,'R3'//10X,3F14.2//)
* * * * *
* * * * *
ADD THE FOLLOWING CARDS AFTER DETERMINATION OF
THE DISCONTINUITY CAPACITANCES FROM CURVES DEVELOPED
BY J. WHINNERY
NOTE: C1, C2, & C3 ARE IN PICO-FARADS/CENTIMETER
* * * * *
* * * * *
C1 = 0.0335
C2 = 0.0525
C3 = 0.0085
Y1 = 1.0/Z3
Y2 = 1.0/Z2
Y3 = 1.0/Z1
Y4 = 1.0/Z0
C11 = C1 * 2.54
C22 = C2 * 2.54
C33 = C3 * 2.54
CD1 = TWOPI * RAD1 * C11
CD2 = TWOPI * RAD1 * C22
CD3 = TWOPI * RAD1 * C33
B1 = (TWOPI * FREQ * CD1)/1000.0
B2 = (TWOPI * FREQ * CD2)/1000.0
B3 = (TWOPI * FREQ * CD3)/1000.0
R1 = -ATAN((B1/Y2)/((Y1/Y2) - 1.0))
R11 = -ATAN((B1/Y2)/((Y1/Y2) + 1.0))
R2 = -ATAN((B2/Y3)/((Y2/Y3) - 1.0))
R22 = -ATAN((B2/Y3)/((Y2/Y3) + 1.0))
R3 = -ATAN((B3/Y4)/((Y3/Y4) - 1.0))
R33 = -ATAN((B3/Y4)/((Y3/Y4) + 1.0))
REFL1 = R1 + R11
REFL2 = R2 + R22
REFL3 = R3 + R33
ALFA1 = -REFL1
ALFA2 = -REFL2 - (2.0 * R11)
ALFA3 = -REFL3 - (2.0 * R11) - (2.0 * R22)
BETA1 = TWOPI/(4.0 * WAVE1)
BETA2 = TWOPI/(4.0 * WAVE2)
X1 = ALFA1/(2.0 * BETA2)
X2 = ALFA2/(2.0 * BETA1)
X3 = ALFA3/(2.0 * BETA1)

```

```

X11 = WAVE2 - X1
X22 = WAVE1 + X1 - X2
X33 = WAVE1 + X2 - X3
WRITE (6,920) X33,X22,X11
920 FORMAT (11X,'THE LENGTHS OF THE TRANSFORMER SECTIONS A
      RE'//20X,'L1
      *,12X,'L2',12X,'L3'//11X,3F14.5///)
* * * * *
* * * * *
NOTE: MAKE SURE THE STOP & END CARD ARE PROPERLY LOCATED
      STOP
      END

```

BIBLIOGRAPHY

1. R. E. Collin, Foundations for Microwave Engineering, pp. 233-237, McGraw Hill, 1966.
2. G. Matthaei, L. Young, and E. Jones, Microwave Filters, Impedance Matching Networks, and Coupling Structures, pp. 204-205, New York: McGrawHill, 1964.
3. D. Lacombe and J. Cohen, "Octave-Band Microstrip DC Blocks," IEEE Trans. Microwave Theory Tech., pp. 555-556, Aug. 1972.
4. M. Ramadan and W. Westgate, "Impedance of Coupled Microstrip Transmission Lines," Microwave Journal, pp. 30-34, July 1971.
5. Hewlett Packard Application Note 935, June 1971.
6. S. Cohn, "Optimum Design of Stepped Transmission-Line Transformers," IRE Trans. Microwave Theory Tech., pp. 16-20, April 1955.